Microporous and Mesoporous Materials 190 (2014) 234–239

Contents lists available at ScienceDirect

Microporous and Mesoporous Materials

journal homepage: www.elsevier.com/locate/micromeso

Carbon dioxide adsorption on MIL-100(M) (M = Cr, V, Sc) metal–organic frameworks: IR spectroscopic and thermodynamic studies

Carlos Palomino Cabello, Paolo Rumori, Gemma Turnes Palomino *

Department of Chemistry, University of the Balearic Islands, 07122 Palma de Mallorca, Spain

ARTICLE INFO

Article history:
Received 13 December 2013
Received in revised form 24 January 2014
Accepted 5 February 2014
Available online 14 February 2014

Keywords:
Carbon capture and storage
Metal-organic frameworks
IR spectroscopy
Thermodynamics

ABSTRACT

Interaction between carbon dioxide and the coordinatively unsaturated Cr(III), V(III) and Sc(III) cationic centers in MIL-100(Cr), MIL-100(V) and MIL-100(Sc), respectively, was studied by means of variable-temperature infrared (VTIR) spectroscopy, a technique that affords determination of standard adsorption enthalpy (ΔH^0) and entropy (ΔS^0) from analysis of IR spectra recorded over a temperature range while simultaneously measuring equilibrium pressure inside a closed IR cell. ΔH^0 was found to be −63, −54 and −48 kJ mol^{-1} for MIL-100(Cr), MIL-100(V) and MIL-100(Sc), respectively, which are among the highest values so far reported for CO_2 adsorption on metal–organic frameworks containing open metal sites. Corresponding values for ΔS^0 resulted to be −210, −198, and −178 J mol^{-1} K^{-1}, thus showing a positive correlation between ΔH^0 and ΔS^0. The observed values of standard adsorption enthalpy are discussed in the broader context of corresponding data reported in the literature for the adsorption of carbon dioxide on other MOFs, as well as on zeolites.

1. Introduction

Carbon-based fossil fuels provide about 80% of the world's energy needs [1], but their combustion is one of the major contributors to the rising levels of carbon dioxide in the atmosphere, and hence to greenhouse effect and its adverse consequences on climate. Despite increasing development of renewable and cleaner energy sources, a fast move away from fossil fuels is unlikely to occur in the mid-term. Consequently, there is a need to develop efficient technologies that could allow us to continue using fossil fuels while reducing CO_2 emissions. Carbon capture and storage (CCS) has been proposed as a means of limiting CO_2 emissions from fossil fuel burning (both in power plants and in other stationary sources), thus mitigating greenhouse effects [2–5].

Current technology for CCS uses mainly liquid amine-based chemical absorbents, but besides the high amount of energy required for regenerating the sorbent, that technology poses some corrosion problems and environmental hazards derived from waste processing, unintentional emissions and accidental release [6–10]. To overcome the drawbacks of amine aqueous solutions, several types of porous adsorbents that can reversibly capture and release CO_2 (in temperature- or pressure-swing cycles) are currently under active investigation as a means to facilitate CO_2 capture from flue gases of stationary sources [11–13]. For cost-effective gas separation, main adsorbent requirements are large adsorption capacity (specially at a low pressure), stability over a large number of adsorption–desorption cycles, fast kinetics, and favorable adsorption thermodynamics, meaning that, in order to facilitate CO_2 capture and release, the corresponding adsorption enthalpy should be neither too low nor too high.

The main types of porous materials currently under active research for CO_2 separation are porous carbons [14,15], zeolites [16–18], and metal–organic frameworks (MOFs) and related compounds [19–24]. Among these, MOFs have attracted significant interest during last years, mainly because metal–organic frameworks and related materials have the advantage of showing a large variety of structural types and chemical composition, which facilitates rational design of chemical synthesis aimed at optimizing gas adsorption properties [25–27]. The large number of structures that can be obtained by changing either the organic linker or the metal endows MOFs with a high versatility for tuning not only pore size and surface area but also adsorption enthalpy, which is a main factor determining preferential gas adsorption, and hence separation, from gas mixtures. MOFs having unsaturated metal cation centers are particularly promising in this context. Removal of the coordinated solvent molecules (which act as terminal ligands for the metal cations embedded within the porous framework) by thermal treatment under a vacuum generates localized carbon dioxide adsorption centers which show enhanced gas–solid

* Corresponding author. Tel.: +34 971 173250; fax: +34 971173426.
E-mail address: g.turnes@uib.es (G.T. Palomino).

http://dx.doi.org/10.1016/j.micromeso.2014.02.015
1387-1811/

interaction energy, thus facilitating selective uptake of CO_2 at a low pressure [19,20,24,28,29].

As a part of a systematic study on the thermodynamics of carbon dioxide adsorption on MOFs having unsaturated metal cations in their framework, and with a view to increase knowledge about prospective carbon dioxide adsorbents for CCS, we report for the first time on variable temperature IR (VTIR) [30,31] studies on the interaction of CO_2 with three members of the MIL-100 isostructural series (MIL-100(Cr), MIL-100(V) and MIL-100(Sc)). MIL-100(M) are mesoporous MOFs that have the chemical composition $M_3O(F/OH)(H_2O)_2[C_6H_3(CO_2)_3]_2{\cdot}nH_2O$. They are metal(III) carboxylates built from trimers of metal octahedra sharing a common oxygen atom which are linked together by trimesate rigid ligands (Fig. 1). There is also a terminal H_2O ligand that can be removed by appropriate thermal treatment, to leave an open (coordinatively unsaturated) cationic site. After solvent removal, the framework structure (which is cubic) shows two types of empty mesoporous cages having free apertures of approx. 2.9 and 3.4 nm, accessible through microporous windows of approx. 0.55 and 0.86 nm, respectively [32–35]. The VTIR method has the advantage of being able to give not only the IR spectroscopic features of gas adsorption complexes, but also the corresponding values of standard adsorption enthalpy and entropy that rule the thermodynamics of the adsorption process, thus allowing a detailed description of the interaction between the gas and the adsorbent which could be very useful in the choice of an optimal adsorbent. The results are discussed in the broader context of relevant data for carbon dioxide adsorption on cation-exchanged zeolites and on other metal–organic frameworks.

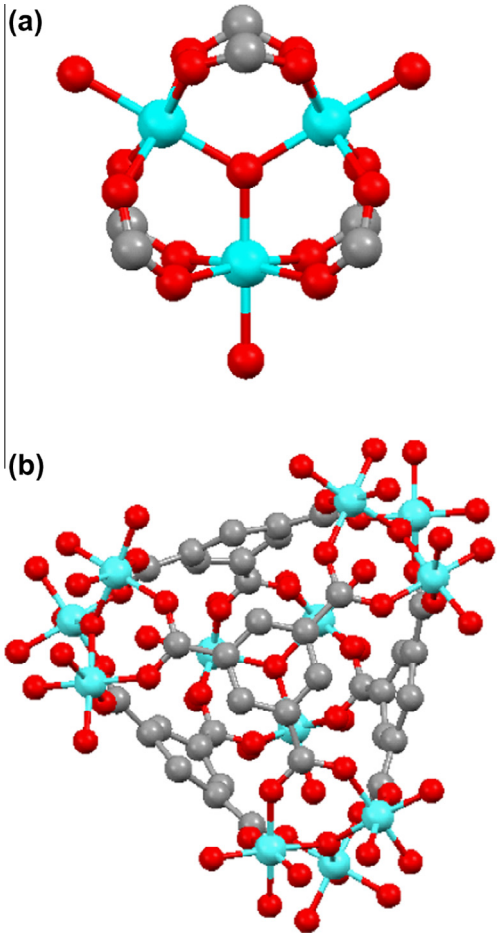

Fig. 1. View of the structure of MIL-100: (a) Trimer of metal octahedra, and (b) schematic tridimensional representation of the supertetrahedra built up from trimers of metal octahedra and trimesate rigid ligands. Metal, carbon and oxygen atoms are depicted as blue, gray and red spheres, respectively. (For interpretation of the references to color in this figure legend, the reader is referred to the web version of this article.)

2. Materials and methods

The MIL-100(M) (M = Cr, V and Sc) samples used were synthesized under solvothermal conditions following procedures reported in the literature [32–35]. The necessary reagents (1,3,5-benzenetricarboxylic acid (Aldrich, 95%), triethyl-1,3,5-benzenetricarboxylate (Aldrich, 97%), chromium(VI) oxide (Sigma–Aldrich, 99%), vanadium(III) chloride (Aldrich, 97%), scandium(III) nitrate hydrate (Aldrich, 99.9%), N,N-dimethylformamide (Scharlau, 99.5%), hydrofluoric acid (Sigma–Aldrich, 40%), ethanol (Scharlau, 96%), and acetone (Scharlau, 99.5%)) were comercially available and used as received.

MIL-100(Sc) was prepared by dissolving 0.204 g of $Sc(NO_3)_3{\cdot}xH_2O$ and 0.084 g of trimesic acid in 15 ml of N,N-dimethylformamide (DMF). The reaction mixture was stirred at room-temperature for 30 min. Then, the mixture solution was transferred into a Teflon-lined autoclave (23 ml) and heated at 423 K for 36 h. After cooling to room temperature, the white powdered product was collected by filtration, washed with DMF, and dried at room temperature. In order to remove the DMF resided in the pores of MIL-100(Sc), the as-synthesized sample was solvothermally treated in ethanol at 373 K for 16 h and then collected by filtration, and dried at room temperature.

MIL-100(V) was synthesized by mixing 0.628 g of VCl_3 and 0.588 g of triethyl-1,3,5-benzenetricarboxylate in 5 ml of deionized water. The synthesis was carried out in a Teflon-lined autoclave (23 ml) at 493 K for 72 h. The product was retained by filtration as a greenish powder and washed with hot ethanol in order to remove the unreacted ligand. Finally it was washed with deionized water and dried at 373 K under air.

MIL-100(Cr) was prepared by mixing 0.5 g of CrO_3, 1.05 g of trimesic acid, and 1.0 ml of a 5 M hydrofluorohydric solution in 24 ml of deionized water. The slurry was stirred for a few minutes at room temperature and then introduced in a Teflon-lined autoclave (45 ml) and set for 96 h at 493 K. The resulting green solid was washed with deionized water and acetone and dried at room temperature under air atmosphere.

The synthesized materials were checked by X-ray powder diffraction. The diffractograms of the obtained products showed in

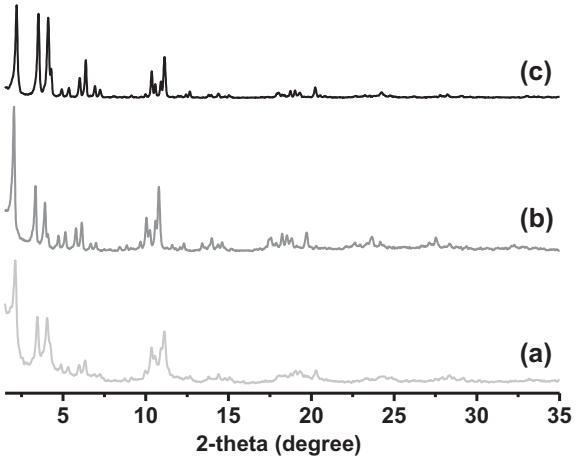

Fig. 2. X-ray diffraction diffractograms (Cu-Kα radiation) of: (a) MIL-100(Cr), (b) MIL-100(Sc) and (c) MIL-100(V) samples.

all cases good cristallinity, and all diffraction lines could be assigned to the corresponding structural types, as shown in Fig. 2.

For infrared spectroscopy, thin self-supported wafers of the MOF samples were prepared and activated (outgassed) in a dynamic vacuum (residual pressure smaller than 10^{-4} mbar) at 553 K for 8 h inside a 2000-A-C AABSPEC cell that allowed us to perform: (i) in situ sample activation, (ii) gas dosage and (iii) variable-temperature IR (VTIR) spectroscopy of adsorbed carbon dioxide while simultaneously recording temperature and equilibrium pressure. A K-thermocouple (in contact with the sample wafer) connected to a digital thermometer (TEMP, XS Instruments) and a capacitance pressure gauge (MKS, Baratron) were used for that purpose; the precision of the measurements was about ±2 K and $\pm 2 \times 10^{-2}$ mbar for temperature and pressure, respectively.

After thermal activation of the sample wafer, the cell was dosed with carbon dioxide and closed, and transmission FTIR spectra were recorded while simultaneously registering the temperature and the gas equilibrium pressure inside the cell. In order to check reproducibility, and also to improve accuracy, the cell was then outgassed and dosed again with CO_2, and a new series of variable temperature IR spectra was recorded. Transmission FTIR spectra were collected, at 3 cm^{-1} resolution, on a Bruker Vertex 80v spectrometer equipped with an MCT cryodetector.

3. Results and discussion

Representative variable-temperature FT-IR spectra of carbon dioxide adsorbed on MIL-100(Cr) in the CO_2 asymmetric stretching region are depicted in Fig. 3a. A main IR absorption band is seen, centered at 2349 cm^{-1}. In agreement with previous results by Férey et al. [33], this band is assigned to the CO_2 asymmetric stretching vibration (ν_3 mode) of carbon dioxide linearly adsorbed onto the coordinatively unsaturated Cr(III) cations of MIL-100(Cr). The corresponding value for the free CO_2 molecule is 2349.3 cm^{-1}. However, carbon dioxide confined in the pores of silicalite is known to show the ν_3 mode at a frequency 8 cm^{-1} smaller than that of free CO_2, i.e., ν_3 = 2341 cm^{-1}, as a result of the confinement effect [36]. Taken this value as the reference, the blue shift in the Cr(III)···CO_2 adsorption complex amounts to 8 cm^{-1}.

IR spectra of CO_2 adsorbed on samples MIL-100(V) and MIL-100(Sc) (Fig. 3b and c) were found to be similar to those obtained for MIL-100(Cr). The spectra are dominated by a band centered at 2348 cm^{-1} ($\Delta\nu$ = 7 cm^{-1}) in the case of MIL-100(V) and at 2352 cm^{-1} ($\Delta\nu$ = 11 cm^{-1}) in the case of MIL-100(Sc) which, by analogy with MIL-100(Cr), is assigned to the ν_3 mode of CO_2 interacting with coordinatively unsaturated V(III) and Sc(III) cations, respectively. In both cases, the spectra show an additional weaker band at approximately 2336 cm^{-1} (also present as a shoulder in the spectra of MIL-100(Cr)), wavenumber value which seems to be insensitive to the nature of the metal cation present in the framework. Similar bands were observed for CO_2 adsorbed on metal–organic frameworks having different structural types [33,37–41], and assigned to CO_2 adsorbed on weaker secondary sites involving organic ligands close to the metal centers [38,40,41]. In agreement with this assignment, the band at around 2336 cm^{-1} is the only one observed when the sample is activated at 325 K, a temperature not enough to remove the water molecules coordinated to the M^{3+} ions (see inset in Fig. 3b).

Comparing the frequencies of the bands corresponding to CO_2 adsorbed on coordinatively unsaturated metal cations, it does not seem to be a direct correlation between the $\Delta\nu$ observed and the polarizing power of the cation suggesting that, as occurs in other microporous materials [16,42,43], dispersion interactions between the adsorbate and the surrounding MOF framework play a significant role in CO_2 adsorption and have an important effect on the vibrational properties of CO_2 adsorbed on these kind of materials.

From the integrated absorbance of a characteristic IR absorption band in spectra taken over a temperature range while simultaneously recording temperature (T) and equilibrium pressure (p) inside a closed IR cell, the standard adsorption enthalpy (ΔH^0) and entropy (ΔS^0) involved in the carbon dioxide adsorption process can be determined following the VTIR method described in detail elsewhere [30,31]. In essence, at any given temperature, the integrated intensity, A, of the corresponding IR absorption band should be proportional to the surface coverage, θ, thus giving information on the activity (in the thermodynamic sense) of both the adsorbed species and the empty adsorption sites, $1-\theta$. Simultaneously, the equilibrium pressure provides similar information for the gas phase. Hence, the corresponding adsorption equilibrium constant, K, can be determined, and the variation of K with temperature yields the corresponding values of adsorption enthalpy and entropy. Assuming Langmuir-type adsorption, we have:

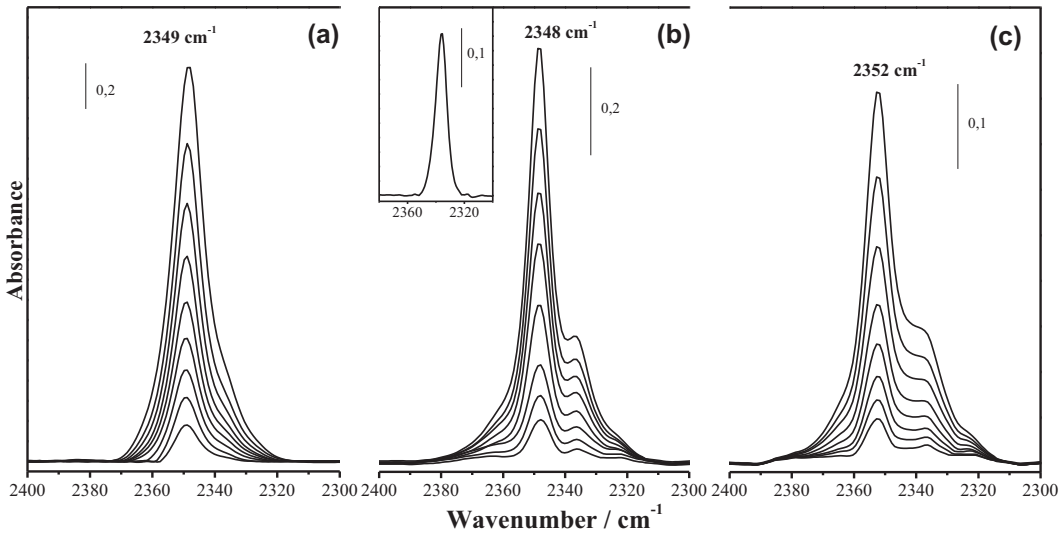

Fig. 3. Representative VTIR spectra (MOF blank subtracted) of CO_2 adsorbed on MIL-100(Cr) (a), MIL-100(V) (b), and MIL-100(Sc) (c). From top to bottom temperature and equilibrium pressure goes from: 320 to 380 K and 7.00 to 7.62 Torr in (a), 303 to 343 K and 6.72 to 7.18 Torr in (b), and 310 to 343 K and 7.80 to 8.10 Torr in (c). Inset: spectrum of CO_2 adsorbed on MIL-100(V) degassed at 325 K.

$$\theta = A/A_M = K(T)p/[1 + K(T)p] \quad (1)$$

where A_M is the integrated intensity corresponding to full coverage ($\theta = 1$). Combination of Eq. (1) with the well known van't Hoff Eq. (2) leads to Eq. (3) below:

$$K(T) = \exp\left(-\Delta H^0/RT\right)\exp\left(\Delta S^0/R\right) \quad (2)$$

$$\ln\left[A/(A_M - A)p\right] = \left(-\Delta H^0/RT\right) + \left(\Delta S^0/R\right), \quad (3)$$

from which ΔH^0 and ΔS^0 are derived, under the usual assumption of their constancy with respect to temperature.

From the whole series of variable temperature IR spectra recorded, and by using (after computer resolution) the integrated intensity of the IR absorption band corresponding to the ν_3 mode of adsorbed CO_2 on the open metal centers, the van't Hoff plots depicted in Fig. 4 were obtained, applying Eq. (3). From those linear plots, the corresponding values of standard adsorption enthalpy and entropy involved in the formation of the corresponding adsorption complexes were determined. The results are shown in Table 1.

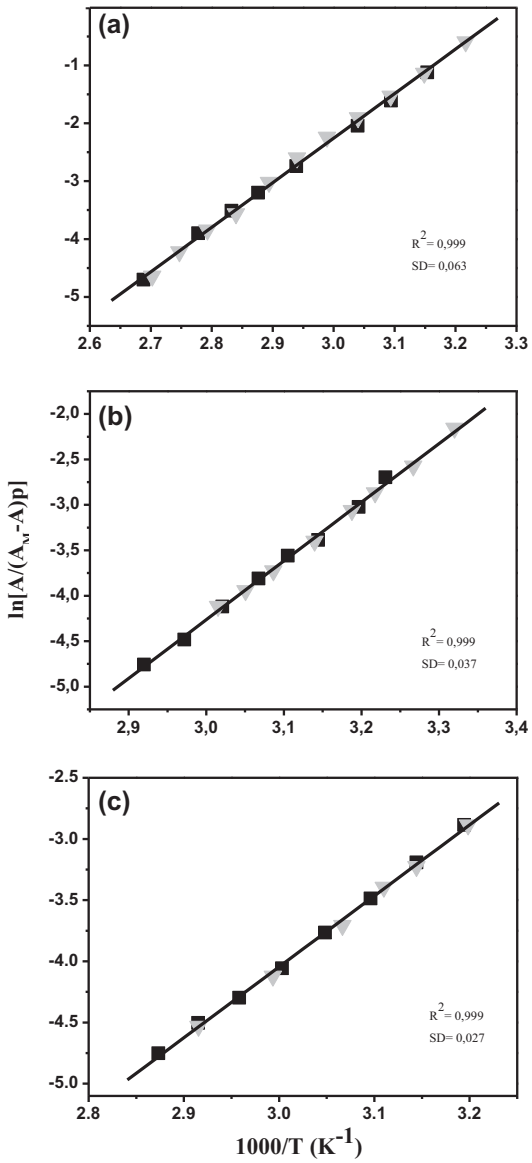

Fig. 4. Plot of the left-hand side of Eq. (3) against the reciprocal of the temperature for carbon dioxide adsorption on MIL-100(Cr) (a), MIL-100(V) (b), and MIL-100(Sc) (c). R, linear regression coefficient and SD, standard deviation. Squares and triangles stand for two different series of spectroscopic measurements.

Regarding enthalpy, the values given herein for CO_2 adsorption in MIL-100(Cr) are in excellent agreement with that reported by Férey et al. [33]. These authors, who investigated the interaction of CO_2 with MIL-100(Cr) by microcalorimetry, reported an adsorption enthalpy of -62 kJ mol^{-1}, which practically coincides, within experimental error, with that of -63 kJ mol^{-1} reported herein. No corresponding value of ΔS^0 was, nevertheless, given in that report. The ΔH^0 values for CO_2 adsorption in MIL-100(V) and MIL-100(Sc) (-54 and -48 kJ mol^{-1}, respectively) are smaller than that shown by CO_2 adsorption in the isostructural MIL-100(Cr) metal–organic framework (-63 kJ mol^{-1}), but still higher than those reported for other MOFs containing coordinatively unsaturated metal cations. In the isostructural series, the CO_2 adsorption enthalpy varies as Cr > V > Sc, showing that the nature of the metal cation and its associated positive charge density affects the binding strength of the initial CO_2 adsorption, which suggest that electrostatic interactions between carbon dioxide molecules and the metal cations also have a significant influence on CO_2 adsorption at low coverage on the metal–organic frameworks studied.

Thermodynamics of CO_2 capture and release is actually ruled by the combined effect of adsorption enthalpy and entropy, and not by ΔH^0 alone. In contrast with calorimetry and determination of isosteric heats, the VTIR method also allows the determination of the standard adsorption entropy, being -210, -198, and -178 J mol^{-1} K^{-1} the values obtained herein for MIL-100(Cr), MIL-100(V), and MIL-100(Sc), respectively. Note that, referring to absolute values, higher values of ΔH^0 correspond to higher values of ΔS^0. Although more data would be desirable for carbon dioxide adsorption on MOFs, the two thermodynamics magnitudes appears to be inter-related and to show a positive correlation. A similar positive correlation was also reported in the literature for a range of chemical processes involving relatively weak interaction forces [44,45], including hydrogen adsorption on cation-exchanged zeolites [46] and on MOFs having coordinatively unsaturated metal cations [47,48]. In general terms, the main argument for such a correlation is that the stronger the interaction between gas molecules and the adsorbing center is, the greater will be the corresponding decrease of motion freedom, which results in an increasing order of the system.

Standard enthalpy and entropy values reported herein for CO_2 adsorption on MIL-100(M) (M = Cr, V, Sc) can be compared with corresponding values for other MOFs having coordinatively unsaturated metal cations and on cation-exchanged zeolites. For this purpose the relevant data are summarized in Table 1. [18,28,29,33,36,43,49–61] Altogether, values of CO_2 adsorption on MOFs containing coordinatively unsaturated metal centers show that ΔH^0 (and ΔS^0 where available) are dependent on the particular MOF and metal center being considered, suggesting that, although the nature of the metal cation influences the energetics of the adsorption process specially at low pressure, carbon dioxide, due to its quadrupolar moment, probably interacts not only with the metal centers but also with the surrounding framework, playing this interaction a significant role in CO_2 adsorption. Proof of it is the fact that some MOFs containing the same cation show different ΔH^0 values, and these values do not always follow the expected trend according to the polarization power of the involved cation, as exemplified by isostructural series of metal–organic frameworks containing different open metal centers. Besides that, standard adsorption enthalpy covers a relatively large range of values, similar to that found by alkaline and some alkaline-earth zeolites, which indicates that, as in that case, this parameter can be conveniently tuned within a wide range by choosing the right MOF topology and the appropriate metal center. Availability of porous

Table 1
Thermodynamic data for carbon dioxide adsorbed on several metal–organic frameworks having coordinatively unsaturated metal cations and zeolites. Error limits for ΔH^0 and ΔS^0 are ±1 kJ mol^{-1} and ±10 J mol^{-1} K^{-1}, respectively.

Adsorbent	$-\Delta H^0$ (kJ mol^{-1})	$-\Delta S^0$ (J mol^{-1} K^{-1})	Method[a]	Refs.
MIL-100(Cr)	63	210	VTIR	This work
MIL-100(V)	54	198	VTIR	This work
MIL-100(Sc)	48	178	VTIR	This work
MIL-100(Cr)	62	–	Cal	[33]
MIL-101(Cr)	44	–	Cal	[33]
$Cu_3(BTC)_2$	29.8	–	Q_{st}	[50]
$Cr_3(BTC)_2$	26.7	–	Q_{st}	[50]
$Ni_3(BTC)_2(Me_2NH)_2(H_2O)$	36.8	–	Q_{st}	[50]
$Mo_3(BTC)_2(DMF)_{0.5}$	25.6	–	Q_{st}	[50]
$[Ru_3(BTC)_2](BTC)_{0.5}$	32.6	–	Q_{st}	[50]
Mg-MOF-74	47	186	VTIR	[43]
	47	–	Q_{st}	[28]
	42	–	Q_{st}	[29,49]
Ni-MOF-74	41	–	Q_{st}	[28]
Co-MOF-74	37	–	Q_{st}	[28]
H-Beta	33	146	VTIR	[51]
H-ZSM-5	31.2	140	VTIR	[52]
H-FER	30.1	124	VTIR	[53]
H-Y	28.5	129	VTIR	[54]
Li-ZSM-5	58.9	–	Q_{st}	[55]
Na-A	42–44[b]	135–140[b]	VTIR	[56]
Na-X	49.1	–	Q_{st}	[57]
Na-FER	45–52[b]	–	Q_{st}	[58]
Na-ZSM-5	50	–	Q_{st}	[57]
	49	–	Cal	[36]
	46.3	–	Q_{st}	[55]
K-FER	40–43[b]	148–152[b]	VTIR	[59]
K-L	42.5	182	VTIR	[60]
K-ZSM-5	44.1	–	Cal	[36]
Rb-ZSM-5	34.9	–	Q_{st}	[55]
Cs-ZSM-5	33	–	Q_{st}	[55]
Ca-A	58	–	Q_{st}	[18]
Ca-CHA	70	–	Q_{st}	[61]

[a] VTIR, variable temperature IR spectroscopy; Cal, calorimetry; Q_{st}, isosteric heat of adsorption.
[b] Depending on the adsorption site.

adsorbents spanning a wide range of ΔH^0 values should facilitate the choice of a suitable material for carbon dioxide capture. In particular, the CO_2 standard adsorption enthalpies of MIL-100(M) metal–organic frameworks studied herein rank among the highest ΔH^0 values so far reported in the literature for MOFs containing coordinatively unsaturated metal cations, suggesting that the incorporation of highly charged metal centers increases CO_2 affinity at low coverage. Although a very high heat of adsorption is not necessarily good in terms of the CO_2 separation application, because of the large energy requirements associated with the regeneration (i.e., desorption) of the materials, these relative high values should enhance CO_2 adsorption capacity and selectivity and facilitate the carbon dioxide adsorption capture and release by means of temperature (or pressure) swing adsorption–desorption cycles.

4. Conclusions

Adsorption of carbon dioxide on three members of the MIL-100 isostructural series (MIL-100(Cr), MIL-100(V) and MIL-100(Sc)) was investigated by means of VTIR spectroscopy, which allowed us to obtain the IR spectra of the corresponding adsorption complex and to determine the adsorption enthalpy and entropy. The results show that, for localized CO_2 adsorption on coordinatively unsaturated metal cations, the standard adsorption enthalpy (ΔH^0) has the value of −63, −54 and −48 kJ mol^{-1} for MIL-100(Cr), MIL-100(V) and MIL-100(Sc), respectively. The corresponding values for the entropy change (ΔS^0) are −210, −198, and −178 J mol^{-1} K^{-1}. These values show a positive correlation between ΔH^0 and ΔS^0 similar to that previously found for hydrogen adsorption on cation-exchanged zeolites and on MOFs having coordinatively unsaturated metal cations. Comparison with corresponding data for other MOFs and zeolites show that the ΔH^0 values for the MIL-100(M) (M = Cr, V, Sc) metal–organic frameworks are among the highest ones reported until now for CO_2 adsorption on metal–organic frameworks containing open metal cations, showing that the incorporation of highly charged metal centers increase CO_2 affinity at low coverage. These values are of the same order of those published for alkali- and some alkaline-earth metal cation-exchanged zeolites, but the large surface area shown by MOFs could be advantageous for gas storage applications.

Acknowledgments

C.P.C. acknowledges the support from the Spanish Ministerio de Educación y Ciencia (pre-doctoral fellowship). The authors acknowledge C. Otero Areán for fruitful discussions.

References

[1] A.J. Hunt, E.H.K. Sin, R. Marriot, J.H. Clark, ChemSusChem 3 (2010) 306–322.
[2] F.M. Orr Jr., Energy Environ. Sci. 2 (2009) 449–458.
[3] R.S. Haszeldine, Science 325 (2009) 1647–1652.
[4] S.A. Rackley, Carbon Capture and Storage, number ed., Butterworth-Heinemann, USA, 2010.
[5] C.W. Jones, E.J. Maginn, ChemSusChem 3 (2010) 861–991.
[6] J. Davison, Energy 32 (2007) 1163–1176.
[7] G.T. Rochelle, Science 325 (2009) 1652–1654.
[8] E.J. Stone, J.A. Lowe, K.P. Shine, Energy Environ. Sci. 2 (2009) 81–91.
[9] K.Z. House, C.F. Harvey, M.J. Aziz, D.P. Schrag, Energy Environ. Sci. 2 (2009) 93–205.
[10] M. Nainar, A. Veawas, Energy Procedia 1 (2009) 231–235.
[11] D.M. D'Alessandro, B. Smit, J.R. Long, Angew. Chem. Int. Ed. 49 (2010) 6058–6082.
[12] Q. Wang, J. Luo, Z. Zhong, A. Borgna, Energy Environ. Sci. 4 (2011) 42–55.

[13] T.C. Drage, C.E. Snape, L.A. Stevens, J. Wood, J. Wang, A.I. Cooper, R. Dawson, X. Guo, C. Satterley, R. Irons, J. Mater. Chem. 22 (2012) 2815–2823.
[14] R. Pini, S. Ottiger, L. Burlini, G. Storti, M. Mazzotti, Int. J. Greenhouse Gas Control 4 (2010) 90–101.
[15] P. Billemont, B. Coasne, G. De Weireld, Langmuir 29 (2013) 3328–3338.
[16] L. Grajciar, J. Čejka, C.O. Areán, G.T. Palomino, P. Nachtigall, ChemSusChem 5 (2012) 2011–2022.
[17] M.R. Hudson, W.L. Queen, J.A. Mason, D.W. Fickel, R.F. Lobo, C.M. Brown, J. Am. Chem. Soc. 134 (2013) 1970–1973.
[18] T.-H. Bae, M.R. Hudson, J.A. Mason, W.L. Quenn, J.J. Dutton, K. Sumida, K.J. Micklash, S.S. Kaye, C.M. Brown, J.R. Long, Energy Environ. Sci. 6 (2013) 128–138.
[19] P.D.C. Dietzel, V. Besikiotis, R. Blom, J. Mater. Chem. 19 (2009) 7362–7370.
[20] J.M. Simmons, H. Wu, W. Zhouab, T. Yildirima, Energy Environ. Sci. 4 (2011) 2177–2185.
[21] Y.S. Bae, R.Q. Snurr, Angew. Chem. Int. Ed. 50 (2011) 11586–11596.
[22] J. Liu, P.K. Thallapally, B.P. McGrail, D.R. Brown, J. Liu, Chem. Soc. Rev. 41 (2012) 2308–2322.
[23] K. Sumida, D.L. Rogow, J.A. Mason, T.M. McDonald, E.D. Bloch, Z.R. Herm, T. Bae, J.R. Long, Chem. Rev. 112 (2012) 724–781.
[24] H.J. Park, M.P. Suh, Chem. Sci. 4 (2013) 685–690.
[25] J.L.C. Rowsell, O.M. Yaghi, Microporous Mesoporous Mater. 73 (2004) 3–14.
[26] G. Ferey, Chem. Soc. Rev. 37 (2008) 191–214.
[27] H. Furukawa, K.E. Cordova, M. O'Keeffe, O.M. Yaghi, Science 341 (2013) (1230444-1–1230444-12).
[28] S.R. Caskey, A.G. Wong-Foy, A.J. Matzger, J. Am. Chem. Soc. 130 (2008) 10870–10871.
[29] D. Yu, A.O. Yazaydin, J.R. Lane, P.D.C. Dietzel, R.Q. Snurr, Chem. Sci. 4 (2013) 3544–3556.
[30] E. Garrone, C.O. Areán, Chem. Soc. Rev. 34 (2005) 846–857.
[31] C.O. Areán, O.V. Manoilova, G.T. Palomino, M.R. Delgado, A.A. Tsyganenko, B. Bonelli, E. Garrone, Phys. Chem. Chem. Phys. 4 (2002) 5713–5715.
[32] G. Férey, C. Serre, C. Mellot-Draznieks, F. Millange, S. Surblé, J. Dutour, I. Margiolaki, Angew. Chem. 116 (2004) 6450–6456 (Angew. Chem. Int. Ed. 43 (2004) 6296–6301).
[33] P.L. Llewellyn, S. Bourrelly, C. Serre, A. Vimont, M. Daturi, L. Hamon, G. De Weireld, J.-S. Chang, D.-Y. Hong, Y.K. Hwang, S.H. Jhung, G. Férey, Langmuir 24 (2008) 7245–7250.
[34] Y.T. Li, K.H. Cui, J. Li, J.Q. Zhu, X. Wang, Y.Q. Tian, Chin. J. Inorg. Chem. 27 (2011) 951–956.
[35] A. Lieb, H. Leclerc, T. Devic, C. Serre, I. Margiolaki, F. Mahjoubi, J.S. Lee, A. Vimont, M. Daturi, J.S. Chang, Microporous Mesoporous Mater. 157 (2012) 18–23.
[36] B. Bonelli, B. Civalleri, B. Fubini, P. Ugliengo, C.O. Areán, E. Garrone, J. Phys. Chem. B 104 (2000) 10978–10988.
[37] S. Bordiga, L. Regli, F. Bonino, E. Groppo, C. Lamberti, B. Xiao, P.S. Wheatley, R.E. Morris, A. Zecchina, Phys. Chem. Chem. Phys. 9 (2007) 2676–2685.
[38] J.T. Culp, A.L. Goodman, D. Chirdon, S.G. Sankar, C. Matranga, J. Phys. Chem. C 114 (2010) 2184–2191.
[39] H. Kim, Y. Kim, M. Yoon, S. Lim, S.M. Park, G. Seo, K. Kim, J. Am. Chem. Soc. 132 (2010) 12200–12202.
[40] B. Li, Z. Zhang, Y. Li, K. Yao, Y. Zhu, Z. Deng, F. Yang, X. Zhou, G. Li, H. Wu, N. Nijem, Y.J. Chabal, Z. Lai, Y. Han, Z. Shi, S. Feng, J. Li, Angew. Chem. Int. Ed. 51 (2012) 1412–1415.
[41] N. Nijem, P. Canepa, L. Kong, H. Wu, J. Li, T. Thonhauser, Y.J. Chabal, J. Phys.: Condens. Matter 24 (2012) 8 (424203).
[42] A. Zukal, A. Pulido, B. Gil, P. Nachtigall, O. Bludský, M. Rubes, J. Čejka, Phys. Chem. Chem. Phys. 12 (2010) 6413–6422.
[43] L. Valenzano, B. Civalleri, S. Chavan, G.T. Palomino, C.O. Areán, S. Bordiga, J. Phys. Chem. C 114 (2010) 11185–11191.
[44] D.H. Williams, M.S. Westwell, Chem. Soc. Rev. 27 (1998) 57–63.
[45] L. Liu, Q.X. Guo, Chem. Rev. 101 (2001) 673–695.
[46] E. Garrone, B. Bonelli, C.O. Areán, Chem. Phys. Lett. 456 (2008) 68–70.
[47] C.O. Areán, S. Chavan, C.P. Cabello, E. Garrone, G.T. Palomino, ChemPhysChem 11 (2010) 3237–3242.
[48] G.T. Palomino, C.P. Cabello, C.O. Areán, Eur. J. Inorg. Chem. (2011) 1703–1708.
[49] J.A. Mason, K. Sumida, Z.R. Herm, R. Krishna, J.R. Long, Environ. Sci. 4 (2011) 3030–3040.
[50] C.R. Wade, M. Dinca, Dalton Trans. 41 (2012) 7931–7938.
[51] M.R. Delgado, C.O. Areán, Energy 36 (2011) 5286–5291.
[52] M. Armandi, E. Garrone, C.O. Areán, B. Bonelli, ChemPhysChem 10 (2009) 3316–3319.
[53] A. Pulido, M.R. Delgado, O. Bludský, M. Rubeš, P. Nachtigall, C.O. Areán, Energy Environ. Sci. 2 (2009) 1187–1195.
[54] C.O. Areán, M.R. Delgado, Appl. Surf. Sci. 256 (2010) 5259–5262.
[55] T. Yamazaki, M. Katoh, S. Ozawa, Y. Ogino, Mol. Phys. 80 (1993) 313–324.
[56] A. Zukal, C.O. Areán, M.R. Delgado, P. Nachtigall, A. Pulido, J. Mayerová, J. Čejka, Microporous Mesoporous Mater. 146 (2011) 97–105.
[57] J.A. Dunne, M. Rao, S. Sircar, R.J. Gorte, A.L. Myers, Langmuir 12 (1996) 5896–5904.
[58] A. Pulido, P. Nachtigall, A. Zukal, I. Domínguez, J. Čejka, J. Phys. Chem. C 113 (2009) 2928–2935.
[59] C.O. Areán, M.R. Delgado, G.F. Bibiloni, O. Bludský, P. Nachtigall, ChemPhysChem 12 (2011) 1435–1443.
[60] C.O. Areán, G.F. Bibiloni, M.R. Delgado, Appl. Surf. Sci. 259 (2012) 367–370.
[61] S.S. Khvoshchev, A.V. Zverev, Zeolites 11 (1991) 742–744.